

# Effect of Polymer Matrix and Metal Species on Facilitated Oxygen Transport in Metalloporphyrin (Oxygen Carrier) Fixed Membranes

Manshi Ohyanagi, Hiroyuki Nishide, Koichi Suenaga, and Eishun Tsuchida\*

Department of Polymer Chemistry, Waseda University, Tokyo 160, Japan.  
Received July 21, 1987

**ABSTRACT:** Facilitated transport of molecular oxygen in membranes (poly(dimethyl siloxane), poly(butyl methacrylate), and poly(methyl methacrylate)) containing cobalt(II) or iron(II)  $\alpha, \alpha', \alpha'', \alpha'''$ -meso-tetrakis(o-pivalamidophenyl)porphyrin as a fixed carrier of oxygen is studied by the combination of oxygen permeability in the membranes and oxygen-binding ability to the metalloporphyrin. The facilitation of oxygen transport is remarkable for the lower upstream pressure, which corresponds to a dual-mode transport model. The facilitation is more enhanced in the polymer matrix with the lower oxygen solubility (according to Henry's law). Although the oxygen-binding affinity of the iron porphyrin is larger than that of the cobalt porphyrin, the facilitation is lower because of its smaller oxygen-binding kinetic constant.

## Introduction

Oxygen permselective polymer membranes have been studied for the production of oxygen-enriched air.<sup>1</sup> Recently a polymer membrane containing a carrier which interacts specifically and reversibly with a gaseous molecule has been remarkably noted as a facilitated transport membrane of the molecule. The concept was first successfully applied to oxygen separation by a liquid membrane<sup>2</sup> containing hemoglobin following application to a liquid membrane<sup>3</sup> containing a cobalt Schiff base complex. However, it is difficult to employ a wet membrane as an oxygen-enriching membrane for air. Therefore, attention has been attracted to the study of a dry polymer membrane containing a metal complex.

The authors previously reported the preparation and the oxygen permselectivity<sup>4</sup> of poly(alkyl methacrylate) membranes containing a cobaltporphyrin complex or a cobalt schiff base complex as a fixed carrier of oxygen. Facilitated oxygen transport was discussed using a dual-mode transport model. However, details such as correlation between the facilitation of oxygen transport and the oxygen-binding ability of metal complexes have not been elucidated. They are necessary to design more efficiently facilitated transport membrane of oxygen. The present paper describes the effect of polymer matrix and metal species on the facilitated transport of oxygen in the polymer membranes containing a metalloporphyrin as a carrier of oxygen. The polymer membranes are prepared by molecularly dispersing cobalt(II) or iron(II)  $\alpha, \alpha', \alpha'', \alpha'''$ -meso-tetrakis(o-pivalamidophenyl)porphyrin complexed with 1-methylimidazole or 1,2-dimethylimidazole in poly(dimethyl siloxane) (PDMS), poly(butyl methacrylate) (PBMA), and poly(methyl methacrylate) (PMMA). The transport behavior of the dissolved oxygen according to a dual mode, Henry's law dissolution and Langmuir adsorption, is analyzed and discussed in terms of the combination of the dual-mode transport model equation<sup>4b,5</sup> and the oxygen-binding kinetic and equilibrium constants of the metalloporphyrin fixed in the membranes.

## Experimental Section

**Materials.** Cobalt(II)  $\alpha, \alpha', \alpha'', \alpha'''$ -meso-tetrakis(o-pivalamidophenyl)porphyrin (CoP) and iron(III)  $\alpha, \alpha', \alpha'', \alpha'''$ -meso-tetrakis(o-pivalamidophenyl)porphyrin bromide (Fe<sup>III</sup>P) were synthesized as in ref 6 and 7. CoP or Fe<sup>III</sup>P were complexed with 1-methylimidazole (Im) or 1,2-dimethylimidazole (MIm) in toluene under nitrogen or argon atmosphere. Toluene solution of the CoPIm and PBMA ( $M_w = 320\,000$ ,  $T_g = 20^\circ\text{C}$ ) or PMMA ( $M_w = 540\,000$ ,  $T_g = 105^\circ\text{C}$ ) were mixed and carefully cast on a Teflon plate under an atmosphere free of oxygen and then dried in vacuo,

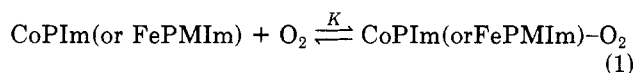
to yield the transparent membranes with a thickness of about 60  $\mu\text{m}$  containing the metalloporphyrin in 2.5 wt %. In the case of Fe<sup>III</sup>P, which does not interact with oxygen, Fe<sup>III</sup>P with MIm in toluene solution was reduced to a bivalent iron porphyrin complex (FePMIm) with oxygen-binding ability by bubbling hydrogen gas in the presence of Pd-C. The PBMA membrane containing FePMIm was cast from the solution in which the catalyst was filtered by a glass filter, under the same conditions as in the case of the CoPIm. PDMS membrane ( $T_g = -123^\circ\text{C}$ ) with a thickness of 200  $\mu\text{m}$  was prepared by using a room temperature vulcanizing silicone rubber (KE-103, Shinetsu Silicone Inc.). The membrane was swollen in the toluene solution containing a large amount of CoPIm, and the solvent was carefully evaporated under an atmosphere free of oxygen. The content of CoPIm thus prepared PDMS membrane was also adjusted to 2.5 wt %.

**Spectroscopic Measurements.** Reversible oxygen-binding to the metalloporphyrin fixed in the membranes was observed with spectral change in the visible absorption, using a high-sensitivity spectrophotometer Shimadzu UV-2000 with a kinetic data processor according to the previously reported method.<sup>4</sup>

**Permeation Measurement.** Oxygen permeation coefficients for various upstream gas pressures were measured with a low-vacuum permeation apparatus in the chamber with stable thermostating (Rika Seiki Inc. Gas permeation apparatus K-315 N-01), as has been reported previously.<sup>4</sup> The permeation coefficient,  $P$ , was calculated from the slope of the steady-state straight line of the permeation curve. The time lag,  $\theta$ , was measured from the crossing point of the steady-state straight line and the abscissa on the permeation curve.

## Results and Discussion

**Effect of Polymer Matrix on Oxygen-Binding Equilibrium and Kinetic Constant of the CoPIm Complex.** The visible absorption spectrum of the deoxy CoPIm complex ( $\lambda_{\text{max}} = 528\text{ nm}$ ) fixed in the transparent membranes is changed to the spectrum with  $\lambda_{\text{max}} = 545\text{ nm}$  assigned to the oxy CoPIm complex ( $\text{O}_2/\text{Co} = 1/1$  adduct) immediately after the exposure of the membranes to oxygen. The oxy-deoxy spectral change is rapid and reversible with isosbestic points at 480, 538, and 667 nm. The oxygen-binding equilibrium constant,  $K$ , of CoPIm in the membranes is determined from Drago's equation and given in Table I.



$K$  for CoPIm in the PDMS membrane is larger than those for CoPIm in the methacrylate polymers. It is considered that the larger solubility of oxygen into the PDMS matrix brings about the larger  $K$ .<sup>8,9</sup> Thermodynamic parameters for oxygen binding are estimated from

Table I  
Oxygen-Binding Rate, Equilibrium Constant,<sup>a</sup> and Its  
Thermodynamic Parameters<sup>b</sup> for the Membranes  
Containing CoPIIm

membrane	$10^3 k_{on}$ , cmHg <sup>-1</sup> s <sup>-1</sup>	$10^2 k_{off}$ , s <sup>-1</sup>	$10^2 K$ , cmHg <sup>-1</sup>	$\Delta H$ , kcal/mol	$\Delta S$ , eu
PDMS	38	10	37	-16	-45
PBMA	1.6	2.3	5.3	-14	-44
PMMA	0.14	0.28	5.2	-13	-40

<sup>a</sup> Data at 25 °C. Membrane thickness: PDMS, 200  $\mu$ m; PBMA, PMMA, 60  $\mu$ m. <sup>b</sup> Data for van't Hoff plots ( $\ln K$  in atm<sup>-1</sup>).

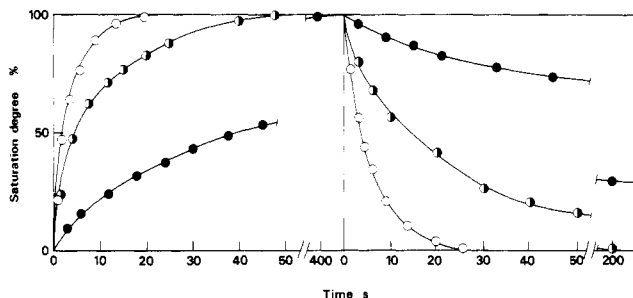


Figure 1. Time course of oxygen ad- and desorption to and from CoPIIm fixed in the following membranes at 25 °C: PDMS (200  $\mu$ m), O; PBMA (60  $\mu$ m), (O); PMMA (60  $\mu$ m), ●. [CoPIIm] = 2.5 wt %.

the temperature dependence of  $K$  and given also in Table I. The enthalpy change becomes more negative with decrease in  $T_g$  of the polymer matrix ( $T_g$ : see Experimental Section). The equilibrium constant and its thermodynamic parameters of the oxygen-binding reaction of CoPIIm fixed in the polymer membrane are affected by both of the oxygen solubility and the dissociation heat in the polymer matrix in these ways.

The oxy-deoxy spectral change occurs very rapidly; e.g., for 60- $\mu$ m-thick rubbery membrane containing 2.5 wt % CoPIIm the oxygen-binding and -dissociation equilibrium is established within a few minutes after exposure to oxygen or in vacuo at 25 °C (Figure 1). The time courses of a saturation degree in the oxygen binding (Figure 1) are analyzed by pseudo-first-order kinetics as reported previously.<sup>4c</sup> These apparent oxygen-binding and -dissociation kinetic constants are larger in the polymer membrane of lower  $T_g$  in the order of the CoPIIm/PDMS, -/PBMA, -/PMMA as shown in Table I because the free volume of a polymer matrix is larger in the membrane with lower  $T_g$  at a constant temperature.

These oxygen-binding parameters are available for the analysis of the oxygen permeation behavior via the fixed carrier, CoPIIm, in the membrane, as described below.

**Effect of Polymer Matrix on Facilitated Transport of Oxygen.** The membrane containing a CoP complex as a fixed carrier sorbs molecular oxygen by a dual mode: Henry's law sorption to the polymer domain and additional Langmuir sorption to the complex. The authors reported<sup>4a,b</sup> that when the CoP complex was fixed in the membrane with its oxygen-binding ability, molecular oxygen was not immobilized to it during the passage through the membrane and diffused via the fixed CoP carrier rapidly. Then, oxygen transport is accelerated by the additional Langmuir mode besides the Henry mode. The oxygen permeation coefficient can be presented as the sum of the Henry mode and the Langmuir mode transport (eq 2).

$$P = k_D D_D + C'_C K D_C / (1 + K p_2) \quad (2)$$

Here,  $P$  is a permeability coefficient,  $k_D$  is a solubility coefficient for Henry's law,  $D_D$  and  $D_C$  are diffusion coefficients for a Henry and a Langmuir-type diffusion,

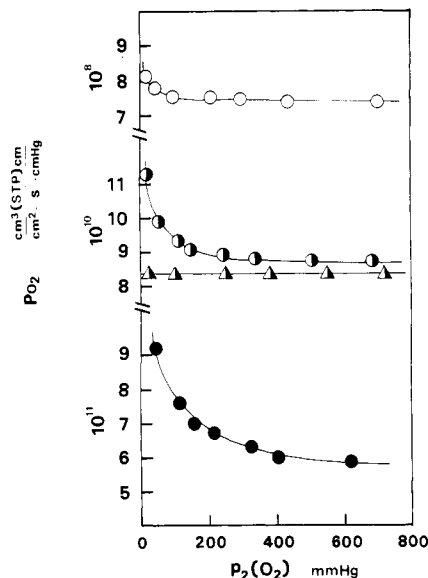


Figure 2. Effect of upstream oxygen pressure on the permeation coefficient in following membranes at 25 °C PDMS, O; PBMA, (O); PMMA, ●; the PBMA membrane containing inert CoPIIm, Δ. [CoPIIm] = 2.5 wt %.

$C'_C$  is a saturated amount of oxygen reversibly bound to a binding site or fixed carrier and may be constant in this case,  $K$  is defined above, and  $p_2$  is an upstream gas pressure. Equation 2 is a function of  $p_2$  and  $P$  increases with a decrease in  $p_2$  when the adsorbed oxygen to the CoP complex is effectively mobile.

Figure 2 shows the effect of  $p_2(O_2)$  on  $P_{O_2}$  in the three membranes containing 2.5 wt % CoPIIm. Each  $P_{O_2}$  increases with the decrease in  $p_2(O_2)$ , which is in accordance with eq 2. The  $p_2(O_2)$  dependency of  $P_{O_2}$  is larger in the membrane with the higher  $T_g$ . This tendency could be explained as follows. In the polymer membrane with smaller oxygen solubility, the ratio of the adsorbed oxygen amount to the complex and the dissolved oxygen amount into the polymer matrix is larger. Therefore, in such a membrane, the fixed carrier according to Langmuir isotherm relatively contributes to the facilitation of oxygen transport in comparison with the case of the membrane with larger oxygen solubility. On the other hand, for higher  $T_g$ ,  $k_D$  is smaller: PDMS membrane,  $3.8 \times 10^{-3}$ ; PBMA membrane,  $9.6 \times 10^{-4}$ ; PMMA membrane,  $5.9 \times 10^{-4}$  [cm<sup>3</sup>(STP)/(cm<sup>3</sup> cmHg)] at 25 °C. From this fact, it is understood that the  $p_2(O_2)$  dependency of  $P_{O_2}$  becomes large in the order of CoPIIm/PDMS, -/PBMA, -/PMMA membrane. Here, the above oxygen solubility coefficients were calculated from the permeability coefficients and the diffusion coefficients  $D$  of the membranes containing the inert Co<sup>III</sup>PIIm complex (2.5 wt %), which does not interact with and does not bind oxygen, based on Fick's and Henry's laws ( $P = k_D D$ ,  $D = L^2/6\theta$ , where  $L$  is the thickness of the membrane and  $\theta$  is time lag).

The facilitated transport of oxygen could be more enhanced by an increase of  $C'_C$ ,  $K$ , and  $D_C/D_D$  related to the oxygen-dissociation rate and by a decrease in  $k_D$ , which is understood by converting eq 2 to  $P = k_D D_D \{1 + D_C K C'_C / (k_D D_D (1 + K p_2))\}$ .

For the membrane containing CoPIIm a time lag,  $\theta$ , in the permeation time course is to be enhanced because the fixed carrier interacts with the penetrant and retards its diffusion in the membrane. The oxygen permeation time lag for the membrane containing CoPIIm is also governed by both the Henry and the Langmuir mode.

$\theta_{O_2}$  for oxygen permeation also depends on  $p_2(O_2)$ , as shown in Figure 3, in the same manner as  $P_{O_2}$ . This be-

Table II  
Dual-Mode Transport Parameters for Membrane Containing CoPIIm

membrane	$D_D$ , $\text{cm}^2/\text{s}$	$D_C$ , $\text{cm}^2/\text{s}$	$F(D_C/D_D)$	$k_D$ , $\text{cm}^3(\text{STP})/(\text{cm}^3 \text{cmHg})$	$C'_C$ , $\text{cm}^3(\text{STP})/\text{cm}^3$
PDMS	$1.9 \times 10^{-5}$	$7.4 \times 10^{-7}$	0.04	$4.0 \times 10^{-3}$	0.1
PBMA	$7.0 \times 10^{-7}$	$1.4 \times 10^{-8}$	0.02	$1.2 \times 10^{-3}$	0.2
PMMA	$2.2 \times 10^{-7}$	$8.3 \times 10^{-8}$	0.04	$2.5 \times 10^{-4}$	0.1

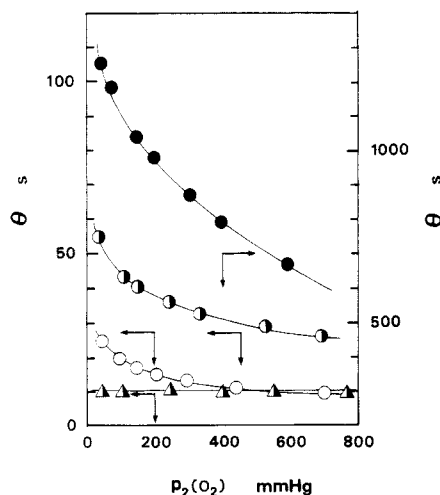


Figure 3. Effect of upstream oxygen pressure on time lag in following membranes at 25 °C: PDMS, ○; PBMA, ●; PMMA, ●; PBMA membrane containing inert CoPIIm, ▲.

havior indicates that oxygen clearly interacts with CoPIIm in the membranes. This is further supported by the results that  $\theta$  is independent of the upstream gas pressures for oxygen permeation in the PBMA membrane containing inert Co<sup>III</sup>PIIm, as shown in Figure 3. Then,  $\theta_{O_2}$  and the  $p_2(O_2)$  dependence of  $\theta_{O_2}$  are larger if the complex is absent. This tendency is also the case for the membrane containing the complex as shown in Figure 3. The  $p_2(O_2)$  dependence of  $\theta_{O_2}$  can be presumed to be larger in the membrane with the smaller oxygen solubility, because the complex in the membrane with a small oxygen solubility contributes to making the oxygen diffusion retard compared with that in the membrane with a large oxygen solubility, in a similar manner as the facilitation of oxygen permeation.

According to the previous method<sup>4b,c</sup> for the determination of the dual-mode parameters, the effect of  $p_2(O_2)$  on  $P_{O_2}$  was analyzed by using eq 2, i.e.,  $P_{O_2}$ s were plotted against  $1/(1 + Kp_2)$ . The effect of  $p_2(O_2)$  on the time lag was also analyzed by using the theoretical equation (eq 3):

$$\frac{6\theta[1 + FR/(1 + y)]^3}{[f_0(y) + FRf_1(y) + (FR)^2f_2(y)]l^2}(Y) = \frac{R}{D_D} + \frac{1 + FRf_3(y) + (FR)^2f_4(y)}{f_0(y) + FRf_1(y) + (FR)^2f_2(y)}(X) \frac{1}{D_D}$$

$$F = D_C/D_D, \quad R = C'_C K/k_D, \quad y = Kp_2, \quad l = \text{thickness of membrane} \quad (3)$$

the  $FR$  value calculated from the slope and the intercept of the linear relationship in eq 3 was substituted in eq 3; the left term ( $Y$ ) was plotted against the right term ( $X$ ). The functions of  $y$ ,  $f_0(y) \sim f_4(y)$  were shown in previous papers.<sup>4b,5</sup>

$D_D$  and  $R (=C'_C K/k_D)$  were calculated from the slope and the intercept of the linear relationship in eq 3, and  $F (=D_C/D_D)$  was obtained from  $FR$  (Table II).

Both  $D_D$  and  $D_C$  decrease with the increase in  $T_g$  because the free volume of the polymer governing the gas diffusivity is reduced with the increase in  $T_g$ . On the other

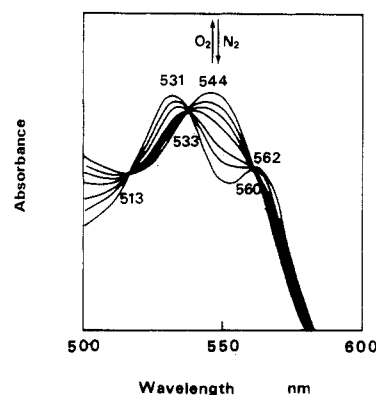


Figure 4. Visible absorption spectral change in oxygen binding to FePMIm/PBMA membrane at 25 °C; [FePMIm] = 2.5 wt %.

Table III  
Oxygen-Binding Rate and Equilibrium Constants<sup>a</sup> for the Membranes Containing Metalloporphyrins

metalloporphyrin	$10^4 k_{on}$ , $\text{cmHg}^{-1} \text{s}^{-1}$	$10^2 k_{off}$ , $\text{s}^{-1}$	$10^2 K$ , $\text{cmHg}^{-1}$
FePMIm	2.3	0.46	5.0
CoPMIm	8.9	4.2	2.1

<sup>a</sup> Data at 25 °C. Membrane thickness, 60  $\mu\text{m}$ .

hand, there is no systematical tendency and few difference in  $F$  for these three membranes.  $F$  is not greatly affected by a polymer matrix. In these polymers  $k_D$  also decreases with the increase in  $T_g$ .  $C'_C$  should be constant in the three membranes because of their same carrier concentration and is in Table II within an error in calculation. The authors believe that  $C'_C$  is critically constant outside of the unavoidable error.

**Reversible Oxygen Binding to the FePMIm Complex Fixed in the Membrane.** The authors will discuss the effect of metal species on facilitated transport of oxygen by comparing FePMIm and CoPMIm as a fixed carrier. Visible absorption spectrum of the deoxy FePMIm complex ( $\lambda_{\text{max}} = 531, 562 \text{ nm}$ ) fixed in the transparent PBMA membrane is changed to the spectrum with  $\lambda_{\text{max}} = 544 \text{ nm}$  assigned to the oxy FePMIm complex ( $O_2/\text{Fe} = 1/1$  adduct) immediately after exposure to oxygen as shown in Figure 4. The oxy-deoxy spectral change is rapid and reversible with isosbestic points at 513, 533, and 560 nm. FeP with an axial base ligand often produces a six coordination complex which has no oxygen-binding site, especially in the solid state. The authors have succeeded, by using 1,2-dimethylimidazole (MIm) as an axial base ligand, in preparing the membrane containing the active FePMIm complex for oxygen binding of which the sixth coordination site is vacant even after the fixation in the membrane. In comparison with CoP complexes, FeP complexes are more easily, irreversibly oxidized during the oxygen-binding reaction because of their lower oxidation potential and because of their lower resistivity against irreversible reaction of their coordinated dioxygen with a water molecule. Thus reversible oxygen binding to FeP complexes has been observed only in absolutely dehydrated solvent except for a few cases.<sup>10</sup> But the FePMIm complex

Table IV  
Dual-Mode Transport Parameters for Membranes Containing Metalloporphyrins

metalloporphyrin	$D_D$ , $\text{cm}^2/\text{s}$	$D_C$ , $\text{cm}^2/\text{s}$	$F(D_C/D_D)$	$k_D$ , $\text{cm}^3(\text{STP})/(\text{cm}^3 \text{cmHg})$	$C'_C$ , $\text{cm}^3(\text{STP})/\text{cm}^3$
CoPMIm	$7.0 \times 10^{-7}$	$2.0 \times 10^{-8}$	0.03	$1.1 \times 10^{-3}$	0.2
FePMIm	$7.0 \times 10^{-7}$	$7.1 \times 10^{-9}$	0.001	$1.2 \times 10^{-3}$	0.2

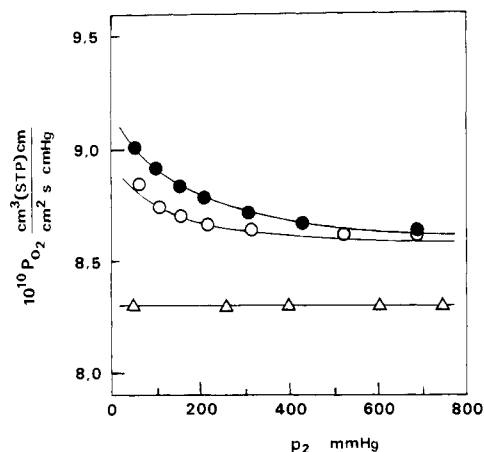


Figure 5. Effect of upstream oxygen pressure on permeation coefficient in the PBMA membranes containing following metalloporphyrins at 25 °C: FeP, O; CoP, ●; Fe<sup>III</sup>P, Δ. [FePMIm], [CoPMIm] = 2.5 wt %.

fixed in the membrane binds oxygen reversibly for a month even under air atmosphere. It is considered that the polymer matrix fixes the FePMIm complex, excludes a water molecule from around the complex, and stabilizes the complex against irreversible oxidation.

The membrane containing the CoPMIm complex was also prepared for the reference of the FePMIm.

$K$  for the oxygen binding of FePMIm in the membrane was determined also by Drago's equation and is given in Table III. The  $K$  of FePMIm in the membrane is larger than that of CoPMIm in analogy with a solution system. The time courses of saturation degree in the oxygen-binding of FePMIm in the membrane were also analyzed by pseudo-first-order kinetics, similarly to the membrane containing CoPIm. These apparent oxygen-binding and -dissociation kinetic constants of FePMIm are smaller than those of CoPMIm as shown also in Table III.

**Effect of Metal Species on Facilitated Transport of Oxygen.** The effect of  $p_2(\text{O}_2)$  on  $P_{\text{O}_2}$  is shown in membranes containing both FePMIm and CoPMIm (Figure 5). Their permeation coefficients increase with the decrease in  $p_2(\text{O}_2)$  which supports the facilitated transport of oxygen by the carriers. The contribution of a fixed carrier becomes larger in the lower  $p_2(\text{O}_2)$  as is easily understood from the dual-mode transport model (eq 2). At the relatively higher  $p_2(\text{O}_2)$ , the  $P_{\text{O}_2}$  values are almost equal in both membranes. But  $P_{\text{O}_2}$  of the membrane containing FePMIm is smaller than that of CoPMIm at lower  $p_2(\text{O}_2)$  as shown in Figure 5. This is one of the evidences that the character of the fixed carrier is critically reflected in the oxygen permeation behavior and could be explained as follows. When  $K$  becomes larger, more part of the Langmuir site, i.e., the complex, is occupied by molecular oxygen; however, the absorbed oxygen is difficult to dissociate from the site if  $k_{\text{off}}$  is much smaller. Probably the smaller mobility of the adsorbed oxygen is governable in comparison with the larger amount of adsorbed oxygen and the facilitation of oxygen permeation in the membrane containing FePMIm is suppressed as shown in Figure 5. Of course,  $P_{\text{O}_2}$  in the membrane containing Fe<sup>III</sup>PMIm

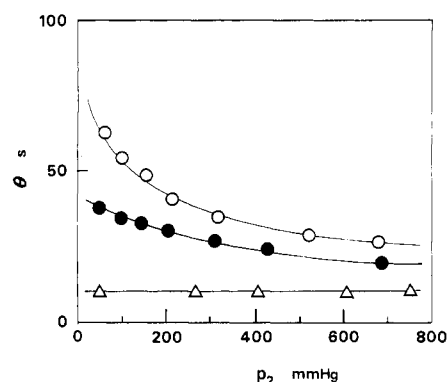


Figure 6. Effect of upstream oxygen pressure on time lag in the PBMA membranes containing following metalloporphyrins at 25 °C: FeP, O; CoP, ●; Fe<sup>III</sup>P, Δ.

which does not interact with oxygen is independent of  $p_2(\text{O}_2)$ .

The effect of  $p_2(\text{O}_2)$  on  $\theta_{\text{O}_2}$  is shown in Figure 6. As predicted from the characters of the FeP and CoP complex compared in Table III,  $\theta_{\text{O}_2}$  in the membrane containing FePMIm is more prolonged in comparison with that of CoPMIm, because of larger oxygen affinity and smaller oxygen kinetic rate constant of FePMIm. The time lag for oxygen permeations in the membrane containing the inert Fe<sup>III</sup>PMIm is independent of  $p_2(\text{O}_2)$ , which supports that the membrane is in a rubbery state. According to the above-mentioned method for determination of dual-mode parameters, the oxygen-permeation coefficient and the time lag were treated.  $D_D$ ,  $k_D$ , and  $C'_C$  are calculated to be almost equal in both membranes (Table IV). This supports the validity of the analysis in terms of dual-mode transport model.  $F$  of the membrane containing FePMIm is about  $1/10$  times the  $F$  for CoPMIm. This difference is based on the smaller  $k_{\text{off}}$  shown in Table III.

For the higher  $T_g$  of the three polymers, the dependence of permeability on upstream oxygen pressure is found to be larger for the lower oxygen solubility in a matrix according to Henry's law. The oxygen-binding affinity of the iron porphyrin is larger in comparison with that of the cobalt one, but the facilitation of oxygen transport is lower than that of the cobalt porphyrin for its small oxygen-binding apparent kinetic constants.

**Acknowledgment.** This work was partially supported by a Grant-in-Aid for Scientific Research on Priority Area of "Macromolecular Complexes" from the Ministry of Education, Science and Culture, Japan.

**Registry No.** PBMA, 9003-63-8; PMMA, 9011-14-7; CoPMIm, 66200-06-4; CoPIm, 53675-32-4; FePMIm, 66200-05-3; O<sub>2</sub>, 7782-44-7.

## References and Notes

- (a) Pusch, W.; Walch, A. *Angew. Chem., Int. Ed. Engl.* **1982**, *10*, 81. (b) Schell, W. J. *J. Membr. Sci.* **1985**, *22*, 217. (c) Comyn, J., Ed. *Polymer Permeability*; Elsevier: New York, 1985. (d) Kesting, R. E. *Synthetic Polymeric Membrane*, 2nd ed.; McGraw-Hill: New York, 1985.
- (a) Scholander, P. F. *Science (Washington, D.C.)* **1960**, *131*, 585. (b) Hemmingsen, E.; Scholander, P. F. *Science (Washington, D.C.)* **1960**, *132*, 1379.

- (3) Johnson, B. M.; Baker, R. W.; Matson, S. L.; Smith, K. L.; Roman, I. C.; Tuttle, M. E.; Lonsdale, H. K. *J. Membr. Sci.* 1987, 31, 31.
- (4) (a) Nishide, H.; Ohyanagi, M.; Okada, O.; Tsuchida, E. *Macromolecules* 1986, 19, 494. (b) Nishide, H.; Ohyanagi, M.; Okada, O.; Tsuchida, E. *Macromolecules* 1987, 20, 417. (c) Tsuchida, E.; Nishide, H.; Ohyanagi, M.; Kawakami, H. *Macromolecules* 1987, 20, 1907. (d) Nishide, H.; Ohyanagi, M.; Funada, Y.; Ikeda, T.; Tsuchida, E. *Macromolecules* 1987, 20, 2312. (e) Nishide, N.; Kuwahara, M.; Ohyanagi, M.; Funada, Y.; Kawakami, H.; Tsuchida, E. *Chem. Lett.* 1986, 43. (f) Nishide, H.; Ohyanagi, M.; Kawakami, H.; Tsuchida, E. *Bull. Chem. Soc. Jpn.* 1986, 59, 3213. (g) Nishide, H.; Ohyanagi, M.; Okada, O.; Tsuchida, E. *Polym. J. Tokyo* 1987, 19, 839.
- (5) Paul, D. R.; Koros, W. J. *J. Polym. Sci., Polym. Phys. Ed.* 1976, 14, 675.
- (6) Collman, J. P.; Brauman, J. I.; Coxsee, K. M.; Halbert, T. R.; Hayes, S. E.; Suslick, K. S. *J. Am. Chem. Soc.* 1978, 100, 2761.
- (7) Collman, J. P.; Gagne, R. R.; Reed, C. A.; Halbert, T. R.; Lang, G.; Robinson, W. T. *J. Am. Chem. Soc.* 1975, 97, 1427.
- (8) Ohyanagi, M.; Nishide, H.; Suenaga, K.; Nakamura, T.; Tsuchida, E. *Bull. Chem. Soc. Jpn.*, in press.
- (9) Herron, N. *Inorg. Chem.* 1986, 25, 716.
- (10) Tsuchida, E.; Nishide, H. *Top. Curr. Chem.* 1986, 132, 63.

## Fast Atom Bombardment Mass Spectrometry Identification of Oligomers Contained in Polysulfides and Their Complexes with Heavy Metals

G. Montaudo\* and E. Scamporrino

*Dipartimento di Scienze Chimiche, Università di Catania, Viale A. Doria, 6-95125 Catania, Italy*

C. Puglisi and D. Vitalini

*Istituto per la Chimica e la Tecnologia dei Materiali Polimerici, Consiglio Nazionale delle Ricerche, Viale A. Doria, 6-95125, Catania, Italy. Received June 1, 1987*

**ABSTRACT:** Fast atom bombardment mass spectrometry (FABMS) was used to identify cyclic oligomers formed in polycondensation reactions leading to aromatic, aliphatic, and aliphatic-aromatic polysulfides. Compounds with a molecular weight up to about 1500 daltons present in the crude polymers were detected without separation. Furthermore, the FABMS technique showed the formation of complexes between the cyclic sulfides contained in the extracted fraction from crude polymers and salts of heavy metals (Ag, Hg, and Cu). In some cases a selectivity of the AgNO<sub>3</sub> toward cyclic sulfides of particular size was also observed.

### Introduction

Recently, we reported the synthesis, separation, and characterization of a series of aromatic,<sup>1</sup> aliphatic,<sup>2</sup> and aliphatic-aromatic<sup>3</sup> cyclic sulfides formed in the polycondensation reaction of dibromo compounds and dithiols.

Gel permeation chromatography (GPC) and electron impact/chemical ionization (EI/CI) mass spectrometry (MS) were used to detect the cyclic oligomers, and a rigorous demonstration of the correspondence of identity among the peaks obtained by these techniques was reported.<sup>1-3</sup>

EI/CI MS is suitable for the detection of low molecular weight compounds contained in the crude polymer samples since they are volatile under the high vacuum of the mass spectrometer at the relatively mild temperatures at which polymers remain undecomposed and therefore undetected.<sup>4,5</sup>

The MS method is based on the direct introduction of the crude sample into the ion source of a mass spectrometer by the direct insertion probe for solid materials. The probe temperature is then gradually increased on a linear program (generally 10 °C/min), and the low molecular weight oligomers, which evaporate undecomposed in the high vacuum of the mass spectrometer, are directly identified by repetitive mass scans.<sup>4</sup> The oligomers are usually detected as separated peaks in the total ion current (TIC) curves before the evolution of the thermal decomposition products originating from the polymer pyrolysis.<sup>4,5</sup>

However, some of the higher molecular weight cyclic sulfides previously investigated by EI/CI MS were too involatile, so that they could not be seen by the MS distillation method.<sup>1-3</sup> As matter of fact, GPC traces always

showed more peaks than TIC curves.<sup>1-3</sup>

Consequently, we have resorted to fast atom bombardment mass spectrometry (FABMS)<sup>6-8</sup> in an attempt to detect and identify, without isolation, the cyclic sulfides formed in the synthesis of some polysulfides.

In the present case we have observed that the FABMS method provides information on all the cyclic oligomers detected by GPC, allowing identification of compounds with a molecular weight up to 1500 daltons (i.e., nearly at the cutoff of our magnet). When the polymers investigated were accurately purified from low molecular weight compounds, no significant peaks were observed in their FAB mass spectra. Instead, the FAB spectra of the mixtures extracted from the polymers were found to be very similar to those obtained for the crude polymers.<sup>9</sup>

Furthermore, we have found that the FABMS technique also allows detection of the complexes among the cyclic sulfides with heavy metals (Ag, Hg, and Cu).

The molecular ions of pure oligomers and those of the corresponding doped sulfides often appear in the spectra with widely differing intensities, therefore providing an analytical tool to detect specific sulfides in a mixture and, conversely, to investigate the selectivity of metals toward macrocyclic sulfides of different size.

### Experimental Section

**Polymer Synthesis and Oligomer Extraction.** Poly(*m*-phenylene sulfide), polymer I (Table I), was prepared by starting from *m*-dibromobenzene and disodium sulfide according to the procedure of Edmonds and Hill.<sup>10</sup>

Poly(hexamethylene sulfide) and poly(trimethylene sulfide), polymers II and III (Table I), were synthesized from the corresponding dithiols and dibromides according to the method de-